

Observation of a muon excess following a gamma-ray burst event detected at the International Space Station

C. R. A. Augusto, V. Kopenkin,* C. E. Navia, M. de Oliveira, and K. H. Tsui

Instituto de Física, Universidade Federal Fluminense, Niterói, Rio de Janeiro 24210-346, Brazil

A. C. Fauth

Instituto de Física Gleb Wataghin, Universidade Estadual de Campinas, Campinas, São Paulo 13081-970, Brazil

T. Sinzi

Rikkyo University, Toshima-ku, Tokyo 171, Japan

(Received 14 June 2012; revised manuscript received 3 April 2013; published 7 May 2013)

On April 24, 2012, at 16:47:14 UT, the Gas Slit Camera (GSC) of the Japanese Monitor of All-sky X-ray Image (MAXI) instrument on the International Space Station detected a short x-ray transient lasting about 34 seconds. The MAXI/GSC transient was most likely a gamma-ray burst (GRB), because of the high Galactic latitude, spectral hardness ratio, and the absence of known bright x-ray sources at the detected position. In addition, the MAXI/GSC transient GRB 120424A coordinates were in the field of view of the inclined Tupi muon telescope located at ground level (3 m above sea level) at (22.9° W, 43.2° S) in the South Atlantic Anomaly region. We report here that the Tupi telescope registered a muon excess with a signal significance 6.2σ within the MAXI/GSC transient time period. Assuming a power law function with a spectral index of $\gamma = -1.54$ in the tail of the primary gamma-ray energy spectrum, we can conclude that the fluence obtained from the muon excess detected by the Tupi telescope is consistent with the preliminary value obtained by the MAXI team. This result agrees with an assumption that the muons were produced in photonuclear reactions in the Earth's atmosphere. In addition, we show also that the South Atlantic Anomaly region can be a favorable place at ground for the detection of the tail of the energy spectrum (the GeV counterpart) of some GRBs.

DOI: [10.1103/PhysRevD.87.103003](https://doi.org/10.1103/PhysRevD.87.103003)

PACS numbers: 98.70.Rz, 94.20.wq, 95.85.Ry, 96.50.sf

I. INTRODUCTION

At random times and from random directions, lasting from milliseconds to many minutes, there are flashes of gamma rays associated with extremely energetic explosions in the Universe. They are known as gamma-ray bursts (GRBs). These bursts are often followed by an afterglow at longer wavelengths (x ray, ultraviolet, optical, infrared, microwave, and radio) that allows us to pinpoint the origin of the GRB. According to the current understanding, the energy at the source of a GRB does not escape from the explosion uniformly but is focused into two oppositely directed jets. Previously it was shown that a substantial fraction of GRBs have photon spectra which extend at least to tens of GeV, at a rate of $\sim 3\text{--}5 \text{ yr}^{-1}$ [1]. In some GRBs the high energy (GeV) component arrives with a considerable delay with respect to the lower energy (keV) component [2,3], while in others, for instance in GRB090926 and GRB090217, the delay was small or negligible [4]. It is generally believed that high energy emission holds clues to the exact mechanisms of GRBs and their afterglow. Numerous emission scenarios can be considered, ranging

from synchrotron and inverse-Compton emissions to photopion production [5–8].

So far, the ground-based Tupi experiment with the muon telescopes has reported extensive observations of small transient events such as energetic solar flares of small scale cataloged as C class, detected in association with the GOES and Fermi spacecrafts [9,10], interplanetary shocks of diverse origins (coronal mass ejection and corotating interaction regions) in association with the ACE and SOHO spacecrafts [11,12], and some possible GeV counterpart of GRBs, such as a delayed connection [13], a prompt connection [14], and an early connection [15]. In the case of GRBs the sea-level muons in gamma showers are mainly produced in a photoproduction process of the primary photon.

The locations of GRBs are mainly detected in real time by spacecrafts (Fermi, Swift, Integral, Wind-Konus). On the ground, various optical telescopes can respond within seconds to signals sent through the Gamma-ray burst Coordinates Network (GCN). Nowadays, among many remarkable detectors in operation there is the Monitor of All-sky X-ray Image (MAXI), the first astronomical payload installed on the Japanese Experiment Module—Exposed Facility (JEM-EF or Kibo-EF) on the International Space Station (ISS) [16]. It can cover about

*Present address: Research Institute for Science and Engineering, Waseda University, Shinjuku, Tokyo 169, Japan.

85% of the whole sky every orbit (~ 90 minutes). MAXI has detected short transient events such as gamma-ray bursts and stellar flares, many in association with other GRB satellite experiments. Here we report new results from the Tupi experiment in association with the MAXI/GSC instrument. On April 24, 2012, MAXI/GSC detected a short x-ray transient lasting about 34 seconds, with the preliminary flux (4–10 keV) of the source 170 ± 30 mCrab [17]. Because of its high Galactic latitude, spectral hardness ratio, and the absence of known bright x-ray sources at the detected position (R.A., Dec) = $(+23.985^\circ, -29.879^\circ)$, this MAXI/GSC transient was probably a gamma-ray burst (GRB 120424A). The Tupi telescope registered a muon excess with a signal significance of 6.2σ within the MAXI/GSC transient time period. We show that from the characteristics of the muon excess detected in the Tupi telescope, this signal can possibly suggest that the muon excess is due to photonuclear reactions in the Earth's atmosphere induced by gamma rays with energies up to more than 10 GeV. Thus, the muon excess observed at the ground could be an indication of the high energy tail of a GRB.

II. THE TUPI TELESCOPE'S SCALER MODE

The Tupi scaler mode consists in recording coincidences rates (scalers) between the two detectors of each telescope. Each counter detector registers signals above the threshold value, corresponding to an energy of ~ 100 MeV deposited by particles (muons) that reach the detector.

Each telescope was constructed on the basis of two detectors (plastic scintillators $50 \text{ cm} \times 50 \text{ cm} \times 3 \text{ cm}$) separated

by a distance of 3 m. Of the six telescopes in operation, we would like to point out two of them that work with a counting rate of up to 30 MHz. One telescope has a vertical orientation, and the other one is oriented at 45 degrees to the vertical (zenith), pointing to the west. Each telescope counts the number of coincident signals in the upper and lower detectors. In addition, each telescope uses a veto or anticoincidence guard system of a third detector close to the two telescopes. For instance, this system allows only the detection of muons traveling close to the axis of the telescope. The telescopes are situated inside a building under two flagstones of concrete, allowing registration of muons with energy threshold around $E_{\text{th}} > 100$ MeV, required to penetrate the two flagstones. Time synchronization is essential for correlating event data in the Tupi experiment. The GPS receiver (Tupi) outputs Universal Time (UT).

The data acquisition system is based on the virtual instrument technique, that is, the analogical signal of each detector is read by a PCI card and all the steps, such as the signal discrimination, coincidence, and counting, are implemented via software. Figure 1 summarizes the situation. The data acquisition diagram is shown in the left figure, and a photograph of the inclined telescope (where the muon excess, in association with the MAXI/GSC transient, has been found) is presented in the right figure.

The effective field of view of each Tupi telescope is estimated to be $\Omega_{\text{eff}} \sim 0.37 \text{ sr} = 0.118\pi$, around eight times smaller than a water Cherenkov tank detector or a typical neutron monitor detector, whose effective field of view is near π . Thus, the narrow solid angle of the Tupi telescopes is another difference in comparison with that of a Cherenkov tank detector or neutron monitor detector.

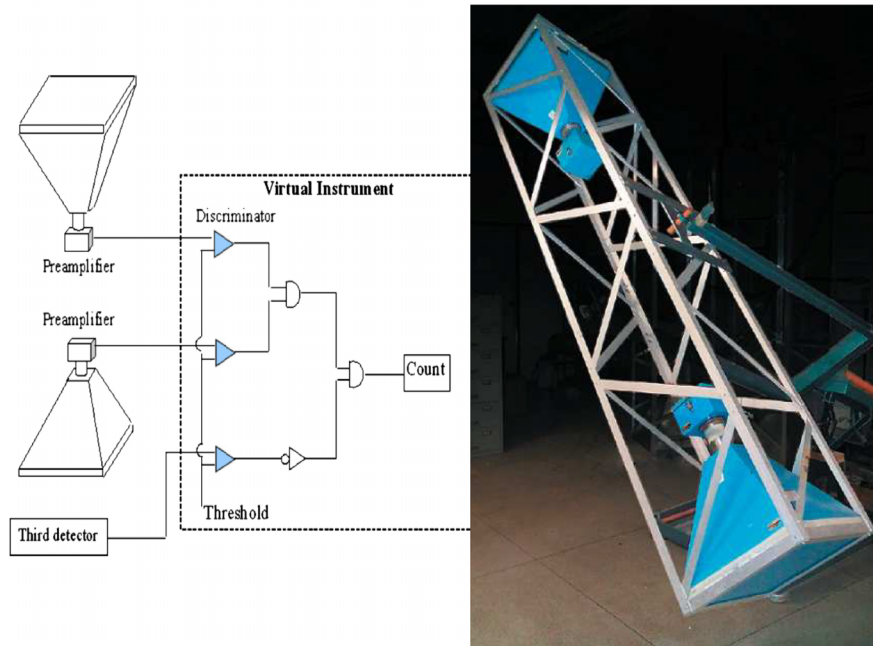


FIG. 1 (color online). Left: General layout of the Tupi telescope, including the logic in the data acquisition system using the virtual instrument technique. Right: Photograph of the Tupi inclined telescope (45 degrees relative to the vertical) and pointing to the west.

III. IS THE SAA REGION FAVORABLE TO GAMMA-RAY ASTRONOMY?

The high sensitivity attained by the Tupi muon telescopes is a consequence (at least in part) of its physical location within the South Atlantic Anomaly (SAA) region.

In the SAA region, it has been shown that the Earth's magnetic field is decreasing at an unprecedented rate and that the region is prone to increased ionospheric ionization by the precipitation of high energy particles from the inner Van Allen belt. Particle precipitation increases the electrical conductivity of the atmosphere.

On the other hand, the expected Stormer rigidity cutoff in the SAA is around 7–9 GV. However, the rigidity observed is much smaller than this value, because in this region, the low magnetic field intensity introduces a sub-cutoff. We have estimated that the cutoff is around 0.8–1.0 GV and this value is consistent with the small cutoff (~ 0.2 GV) observed by the PAMELA spacecraft in the SAA region [18]. Thus, the polar areas and the SAA region are favorable for the observation of charged particles coming from solar transient events, such as solar flares. However, a low rigidity cutoff is not favorable to gamma-ray astronomy, because it tends to increase the background due to low energy cosmic rays. However, at least two factors are extremely favorable for conducting gamma-ray astronomy within the SAA region.

A. The first effect

If a bundle of photons ($E_\gamma > 10$ GeV), for instance, close to the vertical direction, reaches the top of the atmosphere inside the field of view of the vertical telescope, then the muons produced in the atmosphere by photo-production tend to leave the field of view of the telescope. This occurs as the muon travels; it will be shifted by a (horizontal) distance, Δx , in the direction perpendicular to the magnetic field B_T :

$$\Delta x \sim z^2/R = z^2 ce B_T / p, \quad (1)$$

where z is the height of the atmosphere where the muon is generated, and R is the radius of curvature of an (initially) vertical positive muon, traveling downward in the atmosphere with momentum p . In the SAA central region, the magnetic field strength is at least two times smaller than the magnetic field strength outside of the SAA. Consequently, the number of collected muons in a telescope located near the SAA central region is at least two times higher.

Similar aspects of the effect of Earth's magnetic field on low energy gamma-ray detection by atmospheric Cherenkov telescopes has been discussed by the MAGIC team [19].

B. The second effect

Cosmic radiation is the primary source of ions over the oceans and in the upper atmosphere [20]. In the lower

atmosphere, ions are predominantly produced by radiation emitted from radioactive materials in the soil, in building materials [21], and in the air (radon and its daughter products). Cosmic radiation contributes about 10% to the ionization at ground level. However, at higher altitudes, the partitioning shifts drastically both because the radiation from the soil and airborne materials decreases, whereas the intensity of the cosmic radiation increases.

Measurements of atmospheric electrical conductivity are in general difficult to interpret because of a large variety of influencing factors. Therefore, a thorough theoretical and experimental analysis is necessary in order to conduct research in atmospheric electricity.

The variation of the muon intensity at sea level is correlated with the variation of the atmospheric electric conductivity and has a diurnal variation. In a first approximation, the variation of the muon intensity can be described as

$$\frac{\delta I_\mu}{I_\mu} = A_H \delta H + A_\sigma \delta(\log \sigma), \quad (2)$$

where δH and $\delta \sigma$ are the variations of the height of muon production H and the atmospheric conductivity σ , respectively, and A_H is the so-called ‘‘decay’’ coefficient. It is possible to define a new decay coefficient A'_H to take into account the muon intensity variation with atmospheric conductivity, and it is related to the A_H coefficient by the equation

$$A'_H = A_H + A_\sigma \frac{\delta(\log \sigma)}{\delta H}. \quad (3)$$

We would like to point out that, according to Monte Carlo calculations, the altitude of muon production varies widely, and the most probable altitude is in the troposphere ~ 12 km for muons in the GeV energy range.

In the absence of aerosols, the atmospheric electric conductivity [22,23] is given by

$$\sigma \sim eb \left(\frac{q}{\alpha_i} \right)^{1/2}, \quad (4)$$

where q is the ion production rate due to cosmic radiation, α_i is the ion recombination coefficient, e is the charge of an electron, and b is the ionic mobility. Outside of the SAA region, as well as at middle latitudes and in the middle troposphere, the conductivity is of the order of 10^{-12} mho/m [24].

However, according to the NASA AP-8 MAX model, due to the precipitation of particles (mostly protons) at low energy (keV–MeV) coming from the Van Allen inner belt, the particle flux in the central region of the SAA is around 1000 times higher than that outside of the SAA region, as shown in Fig. 2, where data from the NASA AP-8 MAX model are presented.

Thus, an increase of 1000 times in the ion production rate (q) due to particle precipitation in the SAA leads to an increase by a factor of ~ 32 in the electric conductivity of the atmosphere. As the muon decay function A_H is

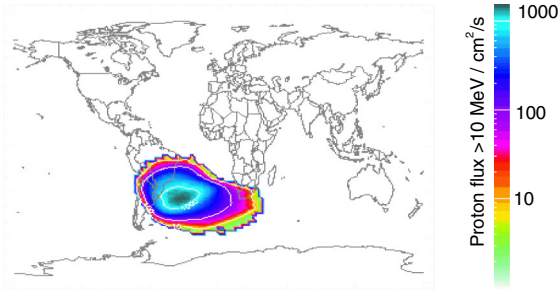


FIG. 2 (color online). Geographic distribution of the particle (mostly protons) precipitation in the MeV energy range coming from the inner Van Allen belt, according to the NASA AP-8 MAX model. The SAA central region is characterized by a high rate of precipitation (more than 1000 times higher than that outside of the SAA region). As a result, there is a high atmospheric ionization in this region.

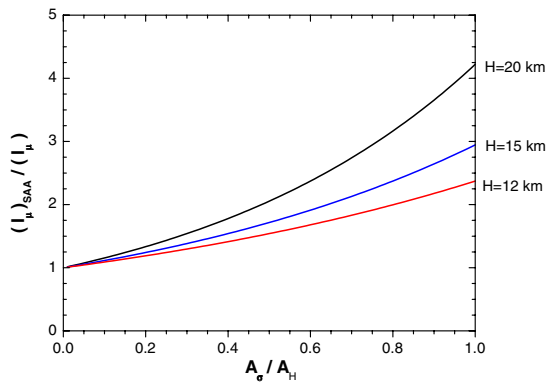


FIG. 3 (color online). Ratio of the muon flux inside the SAA to that outside of the SAA region. Results of the calculations with the same input parameters are presented for different altitudes of muon production in the troposphere.

negative, the increase of the atmospheric conductivity leads to a reduction of the absolute value of the effective muon decay function A'_H , which means that the muon's intensity variation with the atmospheric altitude is less, and the probability of a muon to reach the ground increases.

The above result is very favorable to experimental gamma-ray astronomy using ground detectors, because the muons produced in the atmosphere by gamma rays (photoproduction) have a better chance of reaching the ground: at least two times higher in the SAA region, compared with a region outside of the SAA, as shown in Fig. 3, where the ratio $(I_\mu)_{SAA}/(I_\mu)$ versus different values of A_σ/A_H is plotted. In this case, the conductivity was measured in mhos/m and the height in km.

IV. OBSERVATIONS

On April 24, 2012, at 16:47:14 UT, the MAXI/GSC instrument on the ISS detected a short x-ray transient lasting about 34 seconds within the 40 second triangular

transit response of MAXI/GSC. Assuming that the source flux was constant over the transit, the transient triggered by MAXI/GSC showed the source position at (R.A., Dec) = $(+23.985^\circ, -29.879^\circ) = (01:35:56.40, -29:52:44.0) \times (J2000)$, which has a statistical uncertainty of 16 arc min at the 90% confidence limit and an additional systematic uncertainty of 6 arc min (90% containment radius) [17]. There was no known bright x-ray source at the detected position. The event was at high Galactic latitude. Based on these observations, and also due to the spectral hardness ratio, this MAXI/GSC transient was probably a gamma-ray burst (GRB 120424A).

On April 24, 2012, a sharp peak with a significance of 6.2σ at 68% confidence level was found in the 24 hours of raw data (counting rate at 1 Hz) of the inclined Tupi telescope (see Fig. 1). The Tupi peak with duration 1 s was within the MAXI/GSC time interval. It was possible to recognize this peak in the time profile of the muon counting rate just by the naked eye (see Fig. 4). The Tupi signal significance was calculated according to the bin selection criteria (BSC) algorithm [25,26]. According to this algorithm, the signal statistical significance S in the i th bin is defined as $\sigma_i = (C_i - B)/\sqrt{B}$, where C_i is the measured number of counts in the i th bin and B is the average background count.

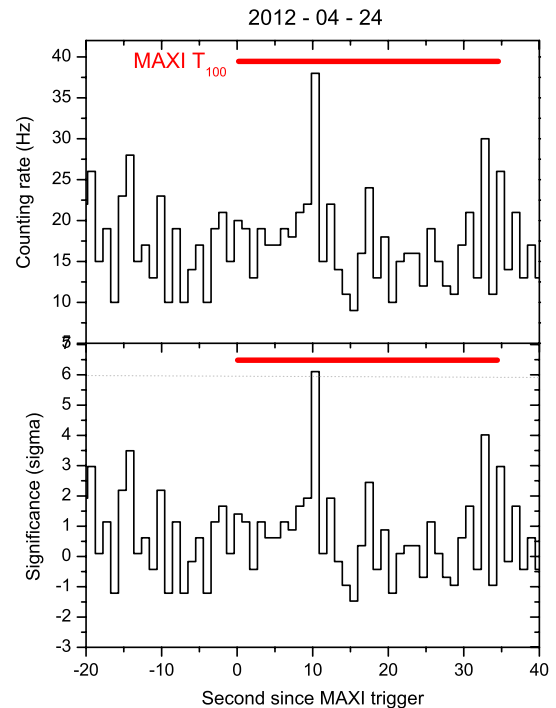


FIG. 4 (color online). Top panel: The raw data observed in the inclined Tupi telescope on April 24, 2012. Bottom panel: Statistical significance (number of standard deviations) of the 1 s binning counting rate observed by the inclined W45 Tupi telescope, both as a function of the time elapsed since the MAXI/GSC transient 120424A trigger time. The red bold lines represent the MAXI event duration.

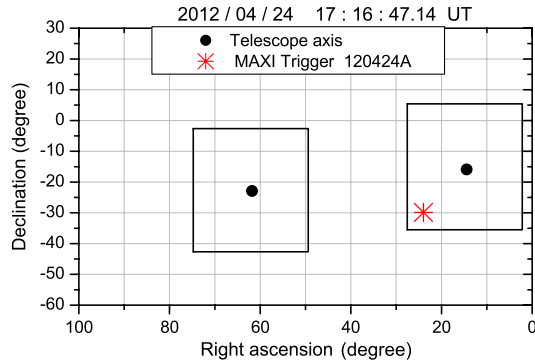


FIG. 5 (color online). The equatorial coordinates of the Tupi telescope's (vertical on the left and inclined W45 on the right) axes (black circles). Squares represent the effective field of view of the telescopes and the asterisk is the position (coordinates) of the MAXI/GSC transient GRB 120424A.

From a cross check with the GCN circular, it was found that the muon excess (peak) occurred 10 seconds after the MAXI/GSC trigger and the coordinates of this MAXI/GSC transient were in the effective field of view of the inclined Tupi telescope as shown in Fig. 5. In addition to that, we found no flare or transient event, as well as no anomalous changes in the atmospheric pressure, temperature, or other known environmental conditions, during the time period close to the signal detection on April 24, 2012.

V. CONFIDENCE ANALYSIS

In order to see the expected background fluctuations, two types of analysis are made. The first is an uncorrelated analysis, and the second is a correlated analysis.

A. Uncorrelated analysis

All the time bins (each of 1 s duration) of the inclined Tupi telescope have been tested by the BSC algorithm. The BSC function follows a Gaussian distribution if there is no signal. A confidence analysis has been made for a 1 hour interval around the MAXI/GSC GRB 120424A trigger time. The results are shown in Fig. 6. From this analysis, it is possible to identify three categories of particles in our observation. First, there is the muon background from the Galactic cosmic ray component that follows a Gaussian distribution (solid line A in Fig. 6). Second, there are muons due to high energy precipitation of trapped and quasitrapped particles in the SAA region (solid line B in Fig. 6). The low energy cosmic ray flux in the SAA region is even higher than the world averages at comparable altitudes. In the present case this component does not exceed $\sim 10\%$ of the Galactic component, and it is consistent with a Gaussian distribution. And third, there is an event with a signal significance of 6.2σ indicated by a vertical arrow. This event corresponds to the muon excess coincident with the MAXI/GSC GRB120424A.

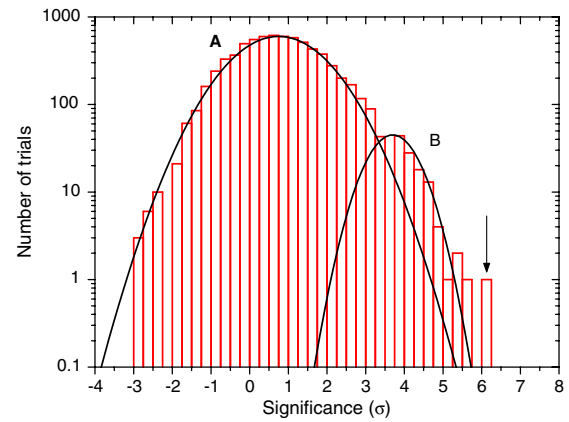


FIG. 6 (color online). Distribution of the fluctuation counting rate for the inclined Tupi telescope (in units of standard deviations), using 1 s time windows inside of a 1 hour interval around the MAXI/GSC GRB 120424A trigger (30 min before and 30 min after the trigger). An arrow indicates the signal significance for the Tupi signal in association with the MAXI/GSC transient. The solid curves (A) and (B) are the expected Gaussian distributions (see text for explanation).

B. Correlated analysis

In the second analysis (shown in Fig. 7) we study the cumulative distribution of the Poisson probability P_i of a signal (the counting rate enhancement) to be a background fluctuation and/or a result of a particle precipitation in the SAA region in the time window $\Delta t = 1$ s during a 1 hour time period, 30 min before and 30 min after the MAXI/GSC trigger. Again, as in Fig. 6, we can see here three

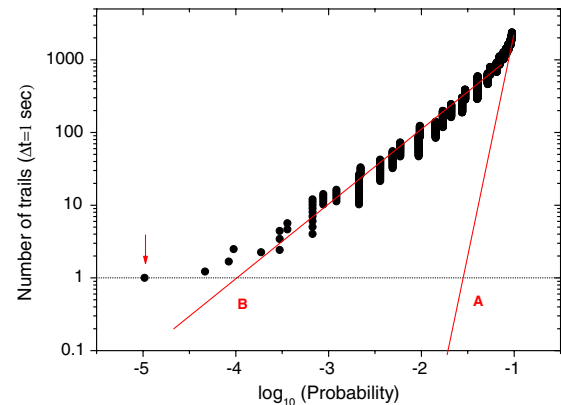


FIG. 7 (color online). Cumulative distribution of the Poisson probability P_i of a signal to be a background fluctuation in the time window of $\Delta t = 1$ s. This is for a 1 hour interval, 30 min before and 30 min after the MAXI/GSC trigger GRB120424A. The solid horizontal line shows one signal in the time window of $\Delta t = 1$ s. The solid line A is the expected distribution under the assumption of background fluctuation only. The solid line B is the expected distribution considering precipitation of the trapped and quasitrapped particles in the SAA area. An arrow indicates the Poisson probability for the Tupi signal (in association with the MAXI/GSC GRB120424A) to be a background fluctuation.

components: the Galactic cosmic ray background fluctuations (solid line A), the fluctuations from particle precipitation in the SAA region (solid line B), and the event indicated by a vertical arrow. From Fig. 7 we can see that the Poisson probability of one signal (counting rate enhancement) to be a background fluctuation in the time window of 1 s is about $\sim 10^{-1.53} = 0.030$, which is 3% (see the crossing point of the horizontal line and the solid line A). The Poisson probability of one signal to be a result of particle precipitation (in the SAA region) is about $\sim 10^{-3.85}$ (0.014%). The arrow in Fig. 7 shows the Tupi signal (associated with the MAXI/GSC event) with probability 10^{-5} (0.001%), which is ten times smaller than the one expected from the particle precipitation and a few thousand times less than the signal expected from the background fluctuations.

VI. SPECTRAL ANALYSIS

The energy spectra of gamma-ray bursts display a diverse phenomenology. The spacecrafts observed gamma rays up to 33 GeV [3]. While some energy spectra can be fitted by a simple power law form over many decades [27], others require a few separate components to explain the high energy emission [28]. Some GRBs do not indicate any cutoff in the spectrum. In most of the cases there can be seen an exact power law solution, which suggests that even higher energy photon emission could be detected. However, above 33 GeV, there have been only upper limit estimations to the GRB flux [29–31]. We assume here that the energy spectrum of gamma rays with energies above 10 GeV, that is, in the high energy region (the tail of the spectrum) of a GRB, can be fitted by a single power law function

$$J(E_\gamma) = A_\gamma \left(\frac{E_\gamma}{\text{GeV}} \right)^\gamma. \quad (5)$$

In this equation there are two unknown quantities, the coefficient A_γ and the spectral index γ . The convolution of a yield function $S(E)$ (number of muons per gamma ray) and the particle spectrum $J(E)$ gives the response function, which is the number of muons in the excess signal generated by the GRB photons during the time period T . This convolution can be expressed as

$$N_\mu = S_{\text{eff}} \times T \int_{E_{\text{min}}}^{\infty} S(E_\gamma) J(E_\gamma, T) dE_\gamma. \quad (6)$$

To obtain the yield function, we have used the results of the fluktuierende kaskade (FLUKA) Monte Carlo simulation [31]. In this framework the minimal effective energy of a gamma ray to produce muons in the atmosphere is ~ 10 GeV. The muon excess allows us to obtain the coefficient A of the primary GRB spectrum as follows:

$$A_\gamma = \left(\frac{N_\mu}{S_{\text{eff}} \times T} \right) \left(\int_{E_{\text{min}}}^{\infty} \left(\frac{E_\gamma}{\text{GeV}} \right)^{-\gamma} S(E_\gamma) dE_\gamma \right)^{-1}. \quad (7)$$

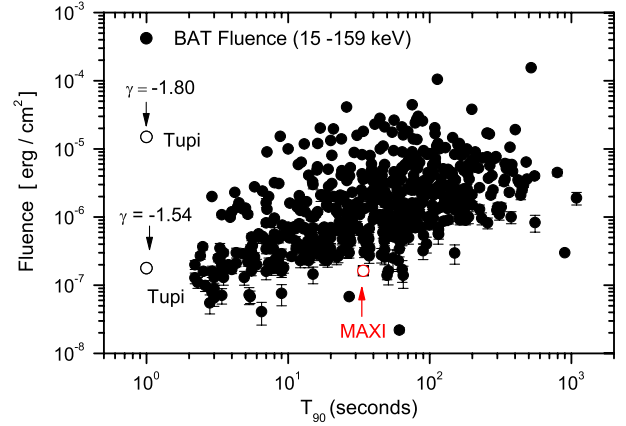


FIG. 8 (color online). Gamma-ray fluence (time integrated intensity) as a function of the burst T90 duration time. The duration parameter T90 is the time over which a burst emits from 5% of its total measured counts to 95%. Solid circles show the Swift BAT gamma-ray fluence and the open circles show the Tupi fluence for two different spectral indices.

The first factor in the right-hand side of the equation is the muon excess flux. However, in order to obtain the coefficient A_γ , it is necessary to know the spectral index. Assuming a power law function with a spectral index of $\gamma = -1.54 \pm 0.62$ for the GRB high energy photons, the parameter $A_\gamma = (1.75 \pm 0.39) \times 10^{-5} \text{ cm}^{-2} \text{ s}^{-1}$ is obtained with 68% C.L.

The Tupi fluence (during 1 second) is estimated as $(1.78 \pm 0.40) \times 10^{-7} \text{ (erg/cm}^2\text{)}$ in the energy range above 10 GeV. This is close to the preliminarily integrated time fluence reported by the MAXI team of $170 \pm 30 \text{ mCrab}$ during 34 seconds, which is equivalent to $1.62 \times 10^{-7} \text{ (erg/cm}^2\text{)}$ in the (4–10 keV) energy range. Figure 8 summarizes the situation.

VII. CONCLUSIONS

(1) We have reported the detection of a muon excess flux (above the background) as $(3.33 \pm 0.74) \times 10^{-3} \text{ cm}^{-2} \text{ s}^{-1}$ with 68% C.L. It can be interpreted as due to photons with energies over 10 GeV from GRB120424A, a transient event with strong features of being the gamma-ray burst observed by the MAXI/GSC instrument on the ISS.

(2) We found that the MAXI/GSC transient coordinates during this simultaneous detection were in the effective field of view of the inclined Tupi telescope.

(3) The low energy cosmic ray flux in the SAA region is even higher than the world average levels at comparable altitudes. This means that in the SAA region and at ground level, the secondary particles in the MeV to GeV energy range have two origins, the Galactic cosmic rays and particle precipitation (trapped and quasitrapped particles). So, an additional background must be considered. Our analysis shows that the Poisson probability of the MAXI/GSC event

GRB120424A to be a result of a particle precipitation is about ten times lower than the expected value.

(4) The overall integrated time fluence of this burst in the energy band from 4 keV to more than 10 GeV is consistent with an assumption of a power law function with a spectral index of $\gamma = -1.54$. In this interpretation, the high energy emission could occur simultaneously with the lower energy emission. In other words, it corresponds to the time occurrence of the muon excess within the T90 time duration of the MAXI transient.

(5) From these observations one can possibly conclude that the detectable high energy emission from GRBs with ground-based experiments (under certain favorable conditions, as in the case of the SAA region) is not a commonplace occurrence, as indeed the Fermi experimental statistics could suggest. In some cases the nondetection may be caused by absorption in the extragalactic background medium (background light), since it is very well known that many GRBs in question do not have well-measured redshifts, while in others an intrinsic spectral cutoff may be a more likely explanation.

(6) This observation indicates that the SAA region can be favorable in the detection of gamma rays from the high energy tail of the spectrum of some GRBs. However, to enjoy the advantages of the SAA region, it is necessary to have a low detection threshold, such as 100 MeV.

ACKNOWLEDGMENTS

This research has made use of the MAXI data provided by RIKEN, JAXA, and the MAXI team. This work is supported by the National Council for Research (CNPq) of Brazil, under Grants No. 306605/2009-0 and No. 01300.077189/2008-6 and Fundacao de Amparo a Pesquisa do Estado do Rio de Janeiro (FAPERJ), under Grants No. 08458.009577/2011-81 and No. E-26/101.649/2011. The authors wish to thank the anonymous referee for assistance, advice, and suggestions. We express our gratitude to European Space Agency and Belgian Institute for Space Aeronomy for providing a user-friendly Web site on The Space Environment Information System (SPENVIS).

-
- [1] P. Meszaros, *Astropart. Phys.* **43**, 134 (2013).
 - [2] K. Hurley *et al.*, *Nature (London)* **372**, 652 (1994).
 - [3] A. A. Abdo *et al.* (Fermi LAT and Fermi GBM Collaborations), *Science* **323**, 1688 (2009).
 - [4] N. Omodei, *Fermi Symposium, Electronic Conference Proceedings Archive* (SLAC National Accelerator Laboratory, Stanford, 2009), <http://www.slac.stanford.edu/econf/>.
 - [5] P. Meszaros and M. J. Rees, *Mon. Not. R. Astron. Soc.* **269**, L41 (1994).
 - [6] P. Kumar and R. B. Duran, *Mon. Not. R. Astron. Soc.* **409**, 226 (2010).
 - [7] J. Katz, *Astrophys. J.* **432**, L27 (1994).
 - [8] D. C. Dermer and A. Atoyan, *Astron. Astrophys.* **418**, L5 (2004).
 - [9] C. R. A. Augusto, C. E. Navia, and M. B. Robba, *Phys. Rev. D* **71**, 103011 (2005).
 - [10] C. E. Navia, C. R. A. Augusto, M. B. Robba, M. Malheiro, and H. Shigueoka, *Astrophys. J.* **621**, 1137 (2005).
 - [11] C. R. A. Augusto, C. E. Navia, H. Shigueoka, K. H. Tsui, and A. C. Fauth, *Phys. Rev. D* **84**, 042002 (2011).
 - [12] C. R. A. Augusto, A. C. Fauth, C. E. Navia, H. Shigeouka, and K. H. Tsui, *Exp. Astron.* **31**, 177 (2011).
 - [13] C. R. A. Augusto, C. E. Navia, M. B. Robba, and K. H. Tsui, *Phys. Rev. D* **78**, 122001 (2008).
 - [14] K. Hurley *et al.*, GCN Circular 9009, <http://gcn.gsfc.nasa.gov/gcn3/9009.gcn3>, 2009.
 - [15] C. R. A. Augusto, V. Kopenkin, C. E. Navia, K. H. Tsui, and T. Sinzi, *Phys. Rev. D* **86**, 022001 (2012).
 - [16] M. Matsuoka *et al.*, *Publ. Astron. Soc. Jpn.* **61**, 999 (2009).
 - [17] M. Serino *et al.*, GCN Circular 13261, <http://gcn.gsfc.nasa.gov/gcn3/13261.gcn3>, 2012.
 - [18] M. Casolino *et al.* (Pamela Collaboration), *Proceedings of the 30th International Cosmic Ray Conference, Mexico City, 2007*, edited by R. Caballero *et al.* (Universidad Nacional Autonoma de Mexico, Mexico City, 2008), Vol. 1, p. 709.
 - [19] R. de los Reyes, E. Ona-Wilhelmi, J. L. Contreras, O. C. Jager, and M. V. Fonseca, *Int. J. Mod. Phys. A* **20**, 7006 (2005).
 - [20] W. A. Hoppel, R. V. Anderson, and J. C. Willett, in *The Earth's Electrical Environment* (National Academy Press, Washington, DC, 1986), pp. 149–165.
 - [21] N. Kamsali, B. S. N. Prasad, and J. Datta, in *Advanced Air Pollution*, edited by F. Nejadkoorki (InTech, Rijeka, Croatia, 2011), pp. 365–390.
 - [22] W. A. Hoppel, *J. Geophys. Res.* **90**, 5917 (1985).
 - [23] W. Gringel, K. H. Käselau, and R. Mühleisen, *Pure Appl. Geophys.* **116**, 1101 (1978).
 - [24] S. P. Gupta, *Adv. Space Res.* **34**, 1798 (2004).
 - [25] I. G. Mitrofanov, D. S. Anfimov, M. S. Briggs, G. J. Fishman, R. M. Kippen, A. S. Kozyrev, M. L. Litvak, C. A. Meegan, W. S. Paciasas, R. D. Preece, and A. B. Sanin, *Astrophys. J.* **603**, 624 (2004).
 - [26] C. R. A. Augusto, C. E. Navia, K. H. Tsui, H. Shigueoka, P. Miranda, R. Ticona, A. Velarde, and O. Saavedra, *Astropart. Phys.* **34**, 40 (2010).
 - [27] A. Abdo *et al.*, *Astrophys. J.* **706**, L138 (2009).
 - [28] G. Aielli *et al.* (ARGO-YBJ Collaboration), *Astrophys. J.* **699**, 1281 (2009).
 - [29] F. Aharonian *et al.*, *Astrophys. J.* **690**, 1068 (2009).
 - [30] R. Atkins *et al.*, *Astrophys. J.* **630**, 996 (2005).
 - [31] A. Fasso and J. Poirier, *Phys. Rev. D* **63**, 036002 (2000).